Fuel 254 (2019) 115639

Contents lists available at ScienceDirect

Fuel

journal homepage: www.elsevier.com/locate/fuel

Full Length Article

Supramolecular nanomaterials with photocatalytic activity obtained via self-assembly of a fluorinated porphyrin derivative

Mahmood D. Aljabri[a], Duong Duc La[b,*], Ratan W. Jadhav[c], Lathe A. Jones[a], Dinh Duc Nguyen[d,e,*], Soon Woong Chang[e], Lam Dai Tran[f], Sheshanath V. Bhosale[c,*]

[a] Centre for Advanced Materials and Industrial Chemistry, School of Science, RMIT University, GPO Box 2476, Melbourne, VIC 3001, Australia
[b] Institute of Chemistry and Materials, Hanoi, Vietnam
[c] School of Chemical Sciences, Goa University, Taleigao Plateau, Goa 403206, India
[d] Institute of Research and Development, Duy Tan University, Da Nang 550000, Vietnam
[e] Department of Environmental Energy Engineering, Kyonggi University, Republic of Korea
[f] Institute for Tropical Technology, Vietnam Academy of Science and Technology, Vietnam

ARTICLE INFO

Keywords:
Porphyrin
Self-assembly
Photocatalysis
Dye degradation
Self-assembled nanomaterials

ABSTRACT

Porphyrin aggregates formed via self-assembly have shown promising photocatalytic activity due to the combination of their optical and morphological properties. The structural and physical properties of porphyrin affect its self-assembly and the properties of the resulting aggregates. The hydrophobicity/hydrophilicity of the porphyrins in solvent mixtures, which affect self-assembly, can be altered by the introduction of fluorine groups. In this work, we report the synthesis of 5,10,15,20-tetrakis(pentafluorophenyl)porphyrin (TPFPP). The differing solubilities of TPFPP in organic and aqueous solutions were exploited to promote the self-assembly of monomeric TPFPP in THF/H_2O solvent mixtures. The effect of the H_2O fraction on the assembly process and resulting morphologies was probed using UV–vis spectroscopy, photoluminescence spectroscopy, and scanning electron microscopy (SEM). It was observed that well-defined TPFPP microrods with a diameter of 1–3 μm and length of 20–100 μm as well as octahedral crystals 30 μm in size were produced with H_2O fractions of 70 and 80%, respectively. These TPFPP aggregates with controlled morphologies exhibited high photocatalytic activity, evident in photocatalytic degradation studies with rhodamine B (RhB) which degraded under visible light irradiation with rate constants of 3.76×10^{-3} (with microrods) and 2.93×10^{-3} min^{-1} (with octahedral crystals). A possible mechanism for the photocatalytic activity of the TPFPP aggregates for RhB degradation was proposed.

1. Introduction

Supramolecular self-assembly is an effective tool for the design and fabrication of functional materials and has been extensively employed to produce soft nanomaterials, such as porphyrin-based nanomaterials, during the last 10 years [1,2]. In particular, π-conjugated porphyrins have attracted great interest as building blocks for functional nanomaterials [3–7]. Porphyrin nanostructures can be formed using bottom-up approaches via self-assembly [8]. The main driving force of the self-assembly process is non-covalent interactions, which consist of hydrogen bonding, van der Waals interactions, electrostatic interactions, aromatic π-π interactions, and coordination bonds. Several self-assembly procedures can be employed, such as surfactant-assisted self-assembly (SAS) [9], ionic self-assembly [10], and reprecipitation [11,12]. Numerous porphyrin nanostructures have been reported with well-defined nanostructures, including spherical structures, nanoprisms, nanotubes, nanofibers, nanorods, nanosheets, nanoclovers, and nanowires [13–20].

Porphyrin nanomaterials exhibit unique physical properties which can be employed in many applications, including optoelectronic devices, energy storage, energy conversion, catalysis, photodynamic therapy, sensors, and photonics [19,21–26]. Recently, the visible-light photocatalytic abilities of porphyrin aggregates have garnered great attention [27–29]. This is influenced by the role of porphyrin-like photoactive molecules as light-harvesting materials in many biological energy transduction processes [30,31]. Therefore, it is of significant interest to design and fabricate supramolecular nanomaterials from porphyrins for applications in photocatalysis. In the past few years,

* Corresponding authors.
E-mail addresses: duc.duong.la@gmail.com (D.D. La), nguyensyduc@gmail.com (D.D. Nguyen), svbhosale@unigoa.ac.in (S.V. Bhosale).

https://doi.org/10.1016/j.fuel.2019.115639
Received 10 March 2019; Received in revised form 4 May 2019; Accepted 11 June 2019
Available online 22 June 2019
0016-2361/

various porphyrin nanostructures have been utilized for photocatalytic degradation under visible light irradiation [11,29,32,33]. For example, Zhong et al. successfully fabricated hierarchical porphyrin nanocrystals such as nanosheets, octahedra, and microspheres and investigated the effect of these morphologies on the photocatalytic activity of the nanocrystals [34]. More recently, we successfully produced nanobelts from tetrakis(4-carboxyphenyl)porphyrin (TCPP) via arginine-induced self-assembly; this photocatalyst was used for the photodegradation of rhodamine B (RhB) dyes under simulated sunlight exposure [34,35]. We also reported the formation of well-dispersed TCPP nanorods on graphene via CTAB-assisted self-assembly [36]. This hybrid nanomaterial exhibited enhanced photocatalytic activity toward RhB dyes. The majority of the previous works related to self-assembly of porphyrins and their applications for photocatalysis have been based on TCPP and its derivatives.

Herein, we reveal the design and synthesis of a new porphyrin derivative, 5,10,15,20-tetrakis(pentafluorophenyl)porphyrin (TPFPP), and investigate its self-assembly properties and photocatalytic performance. Well-defined TPFPP microrods and octahedral crystals were produced via self-assembly in solvent mixtures with controlled H_2O content. These porphyrin aggregates exhibit high photocatalytic performance for RhB degradation under simulated sunlight irradiation. The hypothesized mechanism for photocatalysis via these porphyrin aggregates will be discussed. The results of this work indicate that the self-assembly of supramolecular porphyrin nanomaterials can be controlled through the introduction of F groups in the porphyrin core and the control of the solvent properties during synthesis. This allows for the controlled aggregation of porphyrin monomers into well-defined morphologies, thereby yielding photocatalysts with environmental applications.

2. Results and discussion

The optical properties of the monomeric and assembled TPFPP samples were investigated using UV–vis absorption spectroscopy as shown in Fig. 1 and S1. The UV–vis spectrum of the monomeric TPFPP in pure THF, where the monomer is highly soluble, displayed a strong peak at 407 nm, which is due to the π-π* transition in the porphyrin structure. Upon the addition of increasing amounts of H_2O to the solution (up to a H_2O fraction of 60%), the characteristic peak at 407 nm was only slightly decreased. A further increase in the H_2O fraction above 70% led to a sharp decline of the absorption peak at 407 nm, indicating the initiation of TPFPP self-assembly at this THF/H_2O ratio.

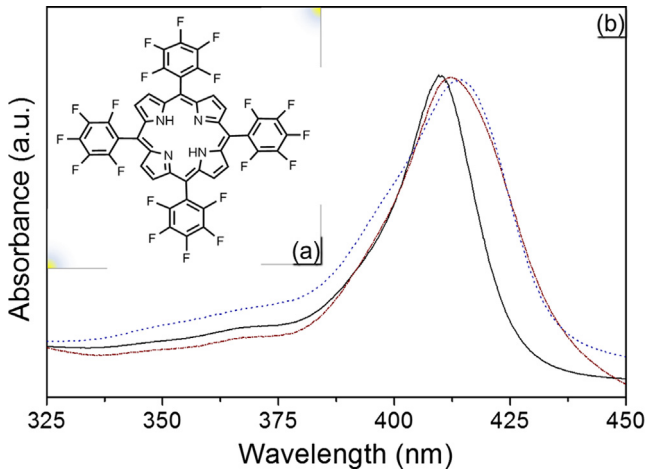

Fig. 1. (a) The structure of the TPFPP monomer used in this investigation. (b) Normalized UV–vis absorption spectra of monomeric TPFPP (black curve), TPFPP in THF upon addition of 70% (blue curve) and 80% (dark red curve) H_2O. (For interpretation of the references to colour in this figure legend, the reader is referred to the web version of this article.)

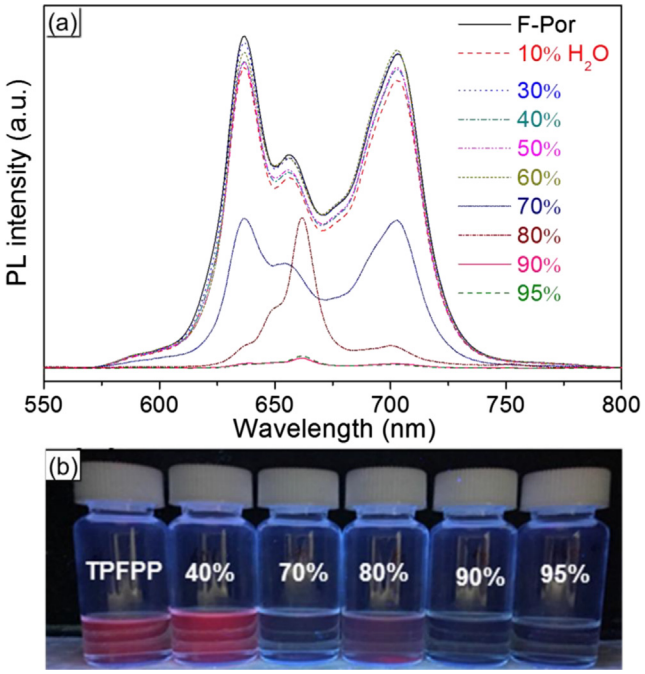

Fig. 2. (a) Photoluminescence spectra of monomeric TPFPP (black line) and TPFPP upon the addition of H_2O from 10 to 95%. (b) Photographic images of TPFPP in THF and THF/H_2O irradiated by UV light (λ_{ex} = 407 nm).

The self-assembly was accompanied by a red-shift in the absorption peak of approximately 7 nm at H_2O fractions of 70 and 80%, which indicates that the supramolecular self-assemblies of the TPFPP monomers are J-aggregates [37,38].

Photoluminescence (PL) spectroscopy was employed to investigate the optical properties of monomeric and aggregate TPFPP (Fig. 2a). The PL spectra of the TPFPP samples were obtained with an excitation wavelength of 407 nm. The PL spectrum of the monomeric TPFPP in pure THF showed three characteristic emission peaks at 637, 657, and 704 nm. When H_2O was added, the fluorescent emission intensity was significantly decreased and was completely quenched at a H_2O fraction of 95%. The quenching effect can also be clearly seen by naked eye (Fig. 2b). The decrease in the emission intensity can be ascribed to the coupling resulting from the spatial packing of the TPFPP molecules upon assembly [34,38].

The morphologies of the TPFPP materials that were self-assembled in THF/H_2O mixtures with various H_2O fractions were observed by scanning electron microscopy (SEM) after the preparation of sample on a silicon surface (Fig. 3, S2–S5). The TPFPP molecules formed microrod structures with diameters of 1–3 μm and lengths of 20–100 μm at 70% H_2O, possibly due to assembly in a head-to-tail fashion. Upon further increase of the H_2O fraction to 80%, octahedral crystals with an average size of approximately 30 μm were observed. However, when the H_2O fraction increased to > 90%, the well-defined morphologies of the assembled TPFPP tended to aggregate, forming a network of fused particles (Fig. 3c and d). This is attributed to the lower solubility of TPFPP at high H_2O fractions, preventing proper nucleation for the self-assembly process during evaporation [34].

Fourier transform infrared spectroscopy (FTIR) analysis was used in order to further confirm the role of non-covalent interactions in the formation of TPFPP nanostructures. Spectra of monomeric and aggregate TPFPP (prepared from THF/H_2O mixtures with H_2O fractions of 70 and 80%) were obtained as shown in Fig. 4. In the FTIR spectrum of TPFPP powder (black solid line), the stretching vibrations at 1044 and 1474 cm^{-1} are attributed to C–F and C=C bonds, respectively. As previously mentioned, the formation of the TPFPP nanostructures is probably due to the π-π stacking of C=C functional groups in the

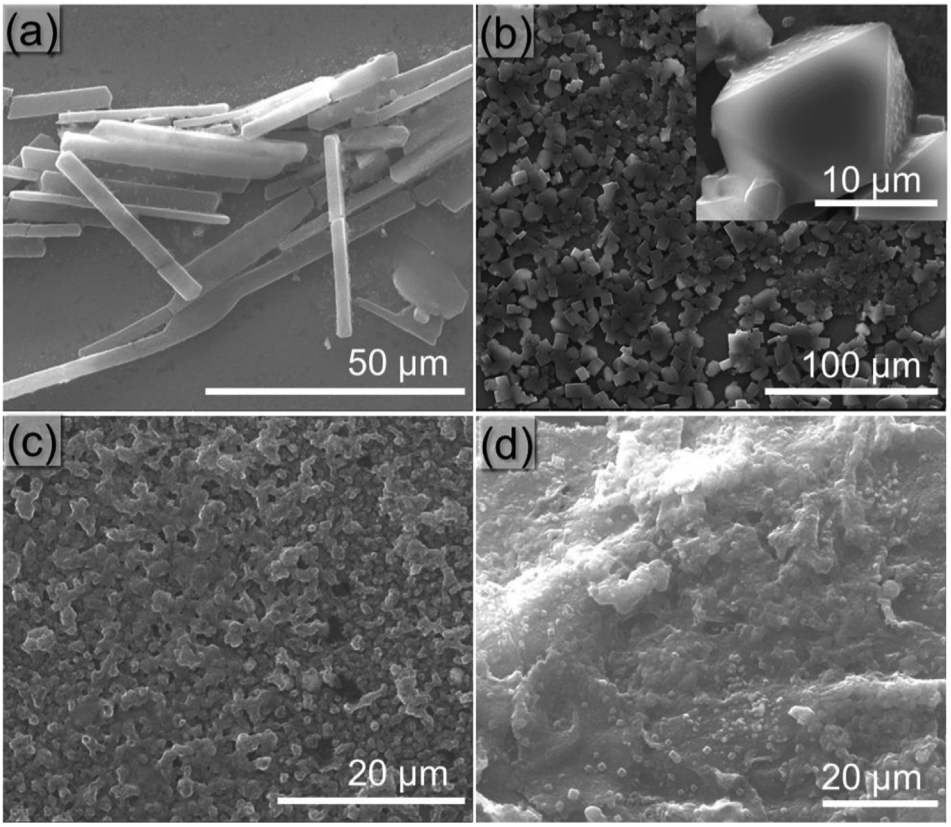

Fig. 3. SEM images depicting the microstructures of TPFPP assembled in (a) f_w = 70%, (b) f_w = 80%, (c) f_w = 90%, and (d) f_w = 95% in THF/H_2O.

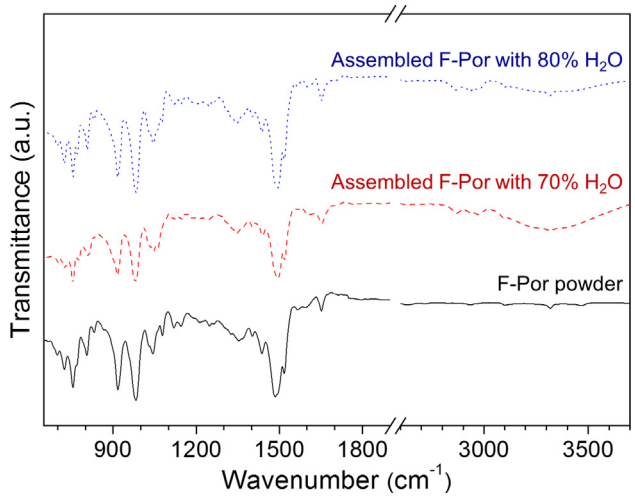

Fig. 4. FTIR spectra of monomeric TPFPP, f_w = 70% microrods, and f_w = 80% octahedral crystals obtained from THF/H_2O.

porphyrin molecules. This is demonstrated by a shift in the stretching vibrations of C=C groups from 1474 cm^{-1} (monomer) to 1493 cm^{-1} (aggregate).

It has been demonstrated that the porphyrin employed here is similar in structure to the naturally photoactive molecule chlorophyll, which exhibits high photocatalytic activity in many biological systems, such as plants and algae [39]. Various assembled porphyrin nanomaterials have previously been used as photocatalysts under visible light irradiation [21,40,41]. The band gap energy of TPFPP microrods and octahedral crystals was determined from the UV–vis spectrum in Fig. 1 to be ca. 2.83 eV, indicating that the photocatalytic properties of TPFPP aggregates can be activated by visible light irradiation, similar to our earlier study of tetracarboxyporphyrin [39].

In this work, the photocatalytic performance of the assembled TPFPP nanomaterials was studied through the degradation of RhB dye under visible light irradiation and compared to the same analysis of the monomeric TPFPP molecule (Fig. 5). As seen in Fig. 5a, when the TPFPP monomer is used as the photocatalyst, the rate of RhB degradation is relatively slow, even after 330 min of irradiation. However, the degradation rate of the RhB dye was significantly increased when porphyrin aggregates were employed instead. The change in the intensity of the absorption peak of the RhB dye at 553 nm was plotted as a function of time in order to study the kinetics of the reaction. The plot of C/C_o vs time is presented in Fig. 5c, where C_o is the initial concentration of dye and C is the dye concentration at time t. It is observed that without photocatalyst, the amount of RhB that is degraded is negligible, indicating that self-sensitized photodegradation of RhB does not occur under these conditions. When monomeric TPFPP was used, a 17% decrease in RhB concentration was observed after 330 min of irradiation. Interestingly, when TPFPP aggregates were employed as the photocatalyst, the RhB dye was significantly degraded with concentration decreases of approximately 71 and 62% for aggregates self-assembled in 70 an 80% H_2O in THF, respectively, indicating that the TPFPP aggregates have greater photocatalytic performance under visible light than the corresponding monomer. The difference in the photocatalytic activity of the two aggregate forms can be attributed to the higher surface area of the microrods compared to that of the octahedral crystals. The kinetics of the photocatalytic reaction were investigated by plotting $\ln(C_t/C_o)$ vs time (where C_o is the intensity of the absorption peak at time zero and C_t is the intensity at time t) (Fig. 5d). The rate constants were determined from this plot. The relative rate constants for RhB degradation under visible light irradiation using TPFPP aggregates (assembled in THF/H_2O mixtures with H_2O fractions of 70 and 80%) were 3.76×10^{-3} and 2.93×10^{-3} min^{-1}, respectively. This further confirms that the TPFPP microrods exhibit higher

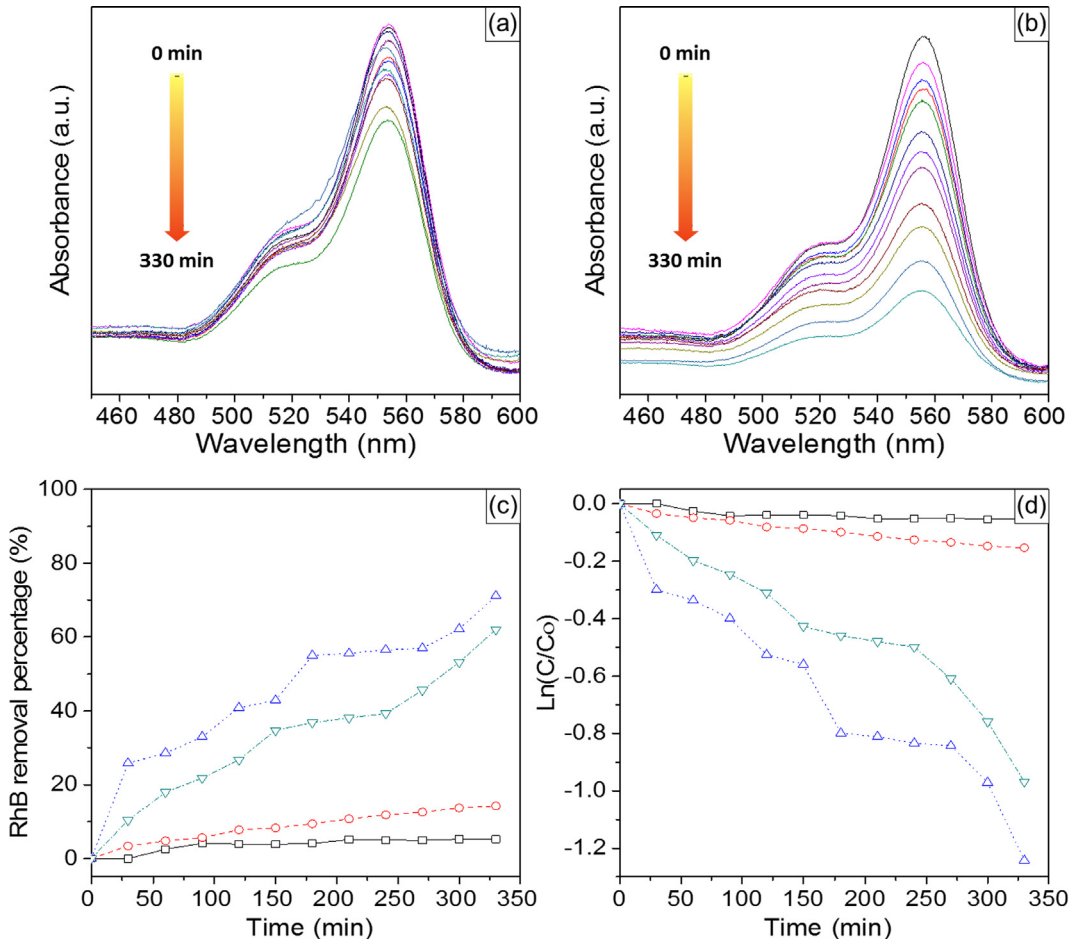

Fig. 5. Photocatalytic performance for RhB degradation with (a) monomeric TPFPP or (b) TPFPP microrods. (c) percentage of RhB degradation and (d) kinetic simulation curve of control (black solid curve), monomeric TPFPP (red dashed curve), TPFPP aggregates with H_2O fraction of 70% (blue dot-dashed curve), and TPFPP aggregates with H_2O fraction of 80% (green dotted curve). (For interpretation of the references to colour in this figure legend, the reader is referred to the web version of this article.)

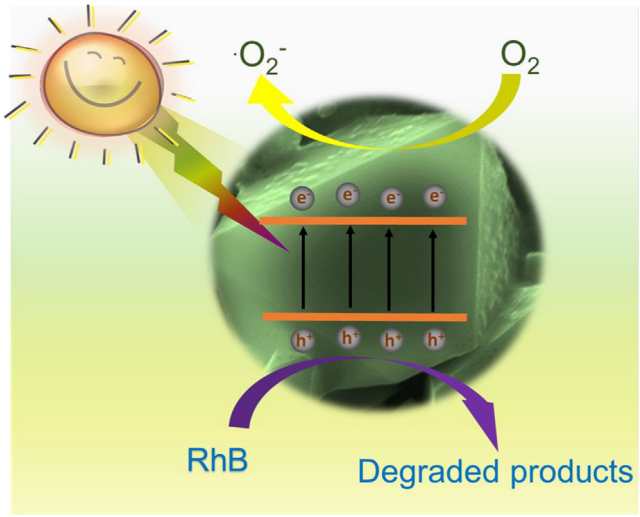

Fig. 6. Possible photocatalytic mechanism of TPFPP aggregates in the degradation of RhB dyes.

photocatalytic activity than the octahedral crystals. These rate constants are also similar to the photocatalytic performance of a well-known self-assembled tetrakis(4-carboxyphenyl)porphyrin reported previously [39,42], and are significantly higher than the standard photocatalyst P-25 Degussa TiO_2 with a relative rate constant of $1.2 \times 10^{-3}\,min^{-1}$ for RhB degradation [37,43]. It is of note that the reaction rate depends on the conditions of the reaction, therefore the rate constants were determined under identical reaction conditions. The higher photocatalytic performance of the porphyrin aggregates compared to the porphyrin monomers is due to the molecular structure of the aggregates, which is similar to photoactive molecules such as chlorophyll, a key molecule in biological light harvesting processes, though the porphyrin aggregates are arranged to achieve better charge separation than that of chlorophyll monomers [44].

Nanostructured porphyrin shows higher photocatalytic activity than amorphous porphyrin due to the improved charge separation resulting from the ordered structure, as compared to the chlorophyll monomer. The porphyrin aggregates act as photoactive molecules, similar to chlorophyll, a porphyrin derivative taking part in many biological energy transduction processes in plants and algae [44]. It has been established that electronic delocalization in J-type aggregates of π-conjugated organic compounds can span over the assembled molecules yielding strong π-π interactions [39], which enables semiconductor properties of such aggregates. Therefore, J-aggregates of porphyrins can be employed as photocatalysts to harvest light and generate electron-hole pairs under visible light irradiation [44,45]. Furthermore, J-aggregates of porphyrin exhibit enhanced charge separation due to excitation-coupled charge transfer processes, which results in improved photocatalytic performance [46]. Based on these results and relevant literature, a possible photocatalytic mechanism for the degradation of RhB dyes by TPFPP aggregates is proposed in Fig. 6, which is similar to

our previously reported mechanism of the photocatalytic activity of self-assembled porphyrins [37–39,42]. Under simulated sunlight irradiation, the TPFPP aggregates harvest photon energy in the visible range. The absorption of photo-energy causes the promotion of electrons from the valence band to the conduction band, generating electron-hole pairs [47]. These electron-hole pairs participate in the degradative redox reaction. The generated holes take part in the oxidative degradation of the RhB dye while the electrons reduce the oxygen of H_2O to $^{\cdot}O_2^-$ on the surface of the TPFPP aggregates.

3. Conclusion

In summary, we have successfully synthesized and characterized a TPFPP molecule that contains hydrophobic groups to control its solubility in THF/H_2O mixtures. This allowed TPFPP to self-assemble into microstructures as the H_2O fraction of the solvent mixture was increased. With a H_2O fraction of 70%, TPFPP assembled to form microrod structures at 1–3 μm in diameter and 20–100 μm in length. Octahedral crystals with an average size of 30 μm were produced by self-assembly of TPFPP in the THF/H_2O mixture with a H_2O fraction of 80%. These porphyrin aggregates exhibited relatively high photocatalytic activity for RhB degradation under simulated sunlight irradiation with rate constants of 3.76×10^{-3} and 2.93×10^{-3} min^{-1} for porphyrin microrods and octahedral crystals, respectively. This study has provided insight into the fabrication of organic semiconductors via self-assembly. In particular, it is determined that control of the porphyrin structure through the introduction of fluorine groups affects the solubility in mixed solvents, allowing for morphological control of the resulting aggregates, which affects their activity in environmental applications.

Acknowledgements

M. D. Aljabri is thankful to Umm Al-Qura University for a full scholarship. S. V. B. acknowledges the University Grant Commission (UGC)-Faculty Research Program (FRP) for providing financial support and an award of professorship. D. D. L. acknowledges the Institute of Chemistry and Materials and NAFOSTED (Grant Code: 104.05-2019.01) for financial support. R. W. J. acknowledges UGC for providing the Junior Research Fellowship. The collaborative research conducted among the groups, institutes and universities of authors are also gratefully acknowledged.

Appendix A. Supplementary data

Supplementary data to this article can be found online at https://doi.org/10.1016/j.fuel.2019.115639.

References

[1] Drain CM, Varotto A, Radivojevic I. Self-organized porphyrinic materials. Chem Rev 2009;109(5):1630–58.
[2] You J-A, Song H, Zhang J, Chen C, Han F. Adsorptive removal of nitrogen-containing compounds from fuel over hierarchical porous aluminosilicates synthesized by kinetic regulation method. Fuel 2019;241:997–1007.
[3] Auwärter W, Écija D, Klappenberger F, Barth JV. Porphyrins at interfaces. Nat Chem 2015;7(2):105–20.
[4] Lee SJ, Hupp JT. Porphyrin-containing molecular squares: design and applications. Chem Rev 2006;250(13):1710–23.
[5] Sakakibara K, Hill JP, Ariga K. Thin-film-based nanoarchitectures for soft matter: controlled assemblies into two-dimensional worlds. Small 2011;7(10):1288–308.
[6] Würthner F, Kaiser TE, Saha-Möller CR. J-aggregates: from serendipitous discovery to supramolecular engineering of functional dye materials. Angew Chem Int Ed 2011;50(15):3376–410.
[7] Lin Y, Wang J, Zhang ZG, Bai H, Li Y, Zhu D, et al. An electron acceptor challenging fullerenes for efficient polymer solar cells. Adv Mater 2015;27(7):1170–4.
[8] Elemans JA, van Hameren R, Nolte RJ, Rowan AE. Molecular materials by self-assembly of porphyrins, phthalocyanines, and perylenes. Adv Mater 2006;18(10):1251–66.
[9] Hoeben FJ, Jonkheijm P, Meijer E, Schenning AP. About supramolecular assemblies of π-conjugated systems. Chem Rev 2005;105(4):1491–546.
[10] Zang L, Che Y, Moore JS. One-dimensional self-assembly of planar π-conjugated molecules: adaptable building blocks for organic nanodevices. Acc Chem Res 2008;41(12):1596–608.
[11] Guo P, Chen P, Ma W, Liu M. Morphology-dependent supramolecular photocatalytic performance of porphyrin nanoassemblies: from molecule to artificial supramolecular nanoantenna. J Mater Chem 2012;22(38):20243–9.
[12] Wang Z, Medforth CJ, Shelnutt JA. Porphyrin nanotubes by ionic self-assembly. J Am Chem Soc 2004;126(49):15954–5.
[13] Lee SJ, Hupp JT, Nguyen ST. Growth of narrowly dispersed porphyrin nanowires and their hierarchical assembly into macroscopic columns. J Am Chem Soc 2008;130(30):9632–3.
[14] Lee SJ, Malliakas CD, Kanatzidis MG, Hupp JT, Nguyen ST. Amphiphilic porphyrin nanocrystals: morphology tuning and hierarchical assembly. Adv Mater 2008;20(18):3543–9.
[15] Gong X, Milic T, Xu C, Batteas JD, Drain CM. Preparation and characterization of porphyrin nanoparticles. J Am Chem Soc 2002;124(48):14290–1.
[16] Hasobe T, Oki H, Sandanayaka ASD, Hideyuki M. Sonication-assisted supramolecular nanorods of meso-diaryl-substituted porphyrins. Chem Commun 2008;6:724–6.
[17] Gao Y, Zhang X, Ma C, Li X, Jiang J. Morphology-controlled self-assembled nanostructures of 5, 15-Di [4-(5-acetylsulfanylpentyloxy) phenyl] porphyrin derivatives. Effect of metal− ligand coordination bonding on tuning the intermolecular interaction. J Am Chem Soc 2008;130(50):17044–52.
[18] Hu J-S, Guo Y-G, Liang H-P, Wan L-J, Jiang L. Three-dimensional self-organization of supramolecular self-assembled porphyrin hollow hexagonal nanoprisms. J Am Chem Soc 2005;127(48):17090–5.
[19] Medforth CJ, Wang Z, Martin KE, Song Y, Jacobsen JL, Shelnutt JA. Self-assembled porphyrin nanostructures. Chem Commun 2009;47:7261–77.
[20] Santos Silva H, Sodero ACR, Korb J-P, Alfarra A, Giusti P, Vallverdu G, et al. The role of metalloporphyrins on the physical-chemical properties of petroleum fluids. Fuel 2017;188:374–81.
[21] Lehn J-M. Toward self-organization and complex matter. Science 2002;295(5564):2400–3.
[22] Xiao J, Qi L. Surfactant-assisted, shape-controlled synthesis of gold nanocrystals. Nanoscale 2011;3(4):1383–96.
[23] Lin C, Zhu W, Yang H, An Q, Ca Tao, Li W, et al. Facile fabrication of stimuli-responsive polymer capsules with gated pores and tunable shell thickness and composite. Angew Chem 2011;123(21):5049–53.
[24] Mousavi M, Hosseinnezhad S, Hung AM, Fini EH. Preferential adsorption of nickel porphyrin to resin to increase asphaltene precipitation. Fuel 2019;236:468–79.
[25] Qian K, Fredriksen TR, Mennito AS, Zhang Y, Harper MR, Merchant S, et al. Evidence of naturally-occurring vanadyl porphyrins containing multiple S and O atoms. Fuel 2019;239:1258–64.
[26] Zhang L, Takanohashi T, Kutsuna S, Saito I, Wang Q, Ninomiya Y. Coordination structures of organically bound paramagnetic metals in coal and their transformation upon solvent extraction. Fuel 2008;87(12):2628–40.
[27] Jang J, Oh JH. Facile fabrication of photochromic dye-conducting polymer core-shell nanomaterials and their photoluminescence. Adv Mater 2003;15(12):977–80.
[28] Cozzoli PD, Pellegrino T, Manna L. Synthesis, properties and perspectives of hybrid nanocrystal structures. Chem Soc Rev 2006;35(11):1195–208.
[29] Chen Y, Li A, Huang Z-H, Wang L-N, Kang F. Porphyrin-based nanostructures for photocatalytic applications. Nanomaterials 2016;6(3):51.
[30] Chen Y, Huang Z-H, Yue M, Kang F. Integrating porphyrin nanoparticles into a 2D graphene matrix for free-standing nanohybrid films with enhanced visible-light photocatalytic activity. Nanoscale 2014;6(2):978–85.
[31] Mandal S, Nayak SK, Mallampalli S, Patra A. Surfactant-assisted porphyrin based hierarchical nano/micro assemblies and their efficient photocatalytic behavior. ACS Appl Mater Interfaces 2014;6(1):130–6.
[32] Uetomo A, Kozaki M, Suzuki S, Yamanaka K-i, Ito O, Okada K. Efficient light-harvesting antenna with a multi-porphyrin cascade. J Am Chem Soc 2011;133(34):13276–9.
[33] Senge MO, MacGowan SA, O'Brien JM. Conformational control of cofactors in nature–the influence of protein-induced macrocycle distortion on the biological function of tetrapyrroles. Chem Commun 2015;51(96):17031–63.
[34] Zhong Y, Wang Z, Zhang R, Bai F, Wu H, Haddad R, et al. Interfacial self-assembly driven formation of hierarchically structured nanocrystals with photocatalytic activity. ACS Nano 2014;8(1):827–33.
[35] Guo P, Chen P, Liu M. One-dimensional porphyrin nanoassemblies assisted via graphene oxide: sheetlike functional surfactant and enhanced photocatalytic behaviors. ACS Appl Mater Interfaces 2013;5(11):5336–45.
[36] La DD, Bhosale SV, Jones LA, Bhosale SV. Arginine-induced porphyrin-based self-assembled nanostructures for photocatalytic applications under simulated sunlight irradiation. Photochem Photobiol Sci 2017.
[37] La DD, Bhosale SV, Jones LA, Revaprasadu N, Bhosale SV. Fabrication of a Graphene@ TiO2@ Porphyrin hybrid material and its photocatalytic properties under simulated sunlight irradiation. ChemistrySelect 2017;2(11):3329–33.
[38] La DD, Rananaware A, Salimimarand M, Bhosale SV. Well–dispersed assembled porphyrin nanorods on graphene for the enhanced photocatalytic performance. ChemistrySelect 2016;1(15):4430–4.
[39] La DD, Hangarge RV, Bhosale SV, Ninh HD, Jones LA, Bhosale SV. Arginine-mediated self-assembly of porphyrin on graphene: a photocatalyst for degradation of dyes. Appl Sci 2017;7(6):643.
[40] Salimimarand M, La DD, Al Kobaisi M, Bhosale SV. Flower-like superstructures of AIE-active tetraphenylethylene through solvophobic controlled self-assembly. Sci Rep 2017;7:42898.

[41] Jang J, Oh JH. Facile fabrication of photochromic dye–conducting polymer core–shell nanomaterials and their photoluminescence. Adv Mater 2003;15(12):977–80.
[42] La DD, Bhosale SV, Jones LA, Bhosale SV. Arginine-induced porphyrin-based self-assembled nanostructures for photocatalytic applications under simulated sunlight irradiation. Photochem Photobiol Sci 2017;16(2):151–4.
[43] La DD, Rananaware A, Thi HPN, Jones L, Bhosale SV. Fabrication of a TiO2@ porphyrin nanofiber hybrid material: a highly efficient photocatalyst under simulated sunlight irradiation. Adv Nat Sci Nanosci Nanotechnol 2017;8(1):015009.
[44] Barber J. Photosynthetic energy conversion: natural and artificial. Chem Soc Rev 2009;38(1):185–96.
[45] Chung WJ, Nguyen DD, Bui XT, An SW, Banu JR, Lee SM, et al. A magnetically separable and recyclable Ag-supported magnetic TiO2 composite catalyst: fabrication, characterization, and photocatalytic activity. J Environ Manage 2018;213:541–8.
[46] Verma S, Ghosh A, Das A, Ghosh HN. Exciton-coupled charge-transfer dynamics in a porphyrin J-aggregate/TiO2 complex. Chem Eur J 2011;17(12):3458–64.
[47] Meadows PJ, Dujardin E, Hall SR, Mann S. Template-directed synthesis of silica-coated J-aggregate nanotapes. Chem Commun 2005;29:3688–90.